quite close to the collapse limit, demonstrating that it is generally important. A current series of monotonic and cyclic tests on damp coal indicates behaviour similar to that of sand.

Stress-dilatancy mechanisms are of potential importance to diverse fields. In steel making, as in any process industry, the reliable provision of material constituents is essential to economic production. Here mass-flow coal hoppers are often duplicated in an attempt to avoid unexpected failures in flow. A proper understanding of stress dilatancy will assist design for reliable flow. The remarkable stiff sand found on the bed of some parts of the North Sea may be explained by the stress-dilatancy response to cyclic loading by the waves. A better understanding will improve estimates of safety margins for offshore oil installations.

We thank Mr F. Cutler, Mr J. Ford and Mr J. Pulsford for making the equipment.

Received 13 June; accepted 27 September 1988.

1. Reynolds, P. *Proc. R. Inst.* **2**, 354-363 (1886).
2. Taylor, D. W. *Fundamentals of soil mechanics* 354-359 (Wiley, New York, 1948).
3. Rowe, P. W. *Proc. R. Soc.* A **269**, 500-527 (1962).
4. Bishop, A. W. *Geotechnique* **16**, 89-130 (1966).
5. Papadopoulos, J. M. thesis, Massachusetts Institute of Technology (1986).
6. Drescher, A. & de Josselin de Jong, G. *J. Mech. Phys. Solids* **20**, 337-351 (1972).
7. Cundall, P. A., Drescher, A. & Strack, O. D. L. *Proc. IUTAM Conf.* Delft 355-370 (1982).
8. Cole, E. R. thesis, Cambridge Univ. (1967).
9. Wong, R. K. S. & Arthur, J. R. F. *Gdotechnique* **35**, 471-481 (1985).
10. Wong, R. K. S. & Arthur, J. R. F. *Geotechnique* **36**, 215-226 (1986).
11. Stroud, M. A. thesis, Cambridge Univ. (1971).
12. Skinner, A. E. *Geotechnique* **19** 150-157 (1969).
13. Rowe, P. W. *Geotechnique* **19** 75-86 (1969).
14. Sharma, Y. K. thesis, London Univ. (1976).

Acoustic and microwave signatures of breaking waves

W. K. Melville, Mark R. Loewen, Francis C. Felizardo, Andrew T. Jessup & M. J. Buckingham*

R. M. Parsons Laboratory, Massachusetts Institute of Technology, Cambridge, Massachusetts 02139, USA
* Radio & Navigation Department,. Royal Aircraft Establishment, Farnborough, Hampshire GU14 6TD, UK

Field experiments have shown that breaking ocean waves may register as discrete events in passive acoustic and active microwave remote sensing measurements of the ocean surface. Using a laboratory model of deep-water wave breaking[1,2] we show here that the noise generated by breaking and the radar cross-section of breaking waves both correlate with the dissipation of surface wave energy. Our results imply that these remote sensing techniques ultimately may be used to measure the dynamics of breaking waves, and are not restricted simply to obtaining the statistics and kinematics of breaking.

It has long been recognized that breaking is an important mechanism for the dissipation of ocean waves, but only recently has its larger role in the dynamics of the upper ocean begun to be recognized and quantified. Until recently, progress has been slow because of the difficulty of measuring spatially and temporally intermittent events in what is often a hostile environment. These difficulties have led a number of investigators to seek other means of measuring breaking, using microwave or acoustic techniques. Thorpe[3] has pioneered the use of active acoustics to image the bubble clouds generated by breaking and to use them as tracers of the boundary layer. Farmer and Vagle[4] have used passive acoustics to identify breaking events as one of the major sources of surface noise in the ocean, and have shown that the acoustics contain information about the wave field. Phillips[5] has suggested that a significant component of microwave scattering from the ocean surface may be due to short episodes of high scattering cross-section ('sea spikes') associated with breaking waves. It remains, nevertheless, to establish whether there are quantitative correlations between the dynamic and kinematic variables that describe breaking and the microwave and acoustic signatures, that is, whether breaking can be quantified, rather than merely detected, by these remote sensing techniques. Here we present evidence to show that this is the case.

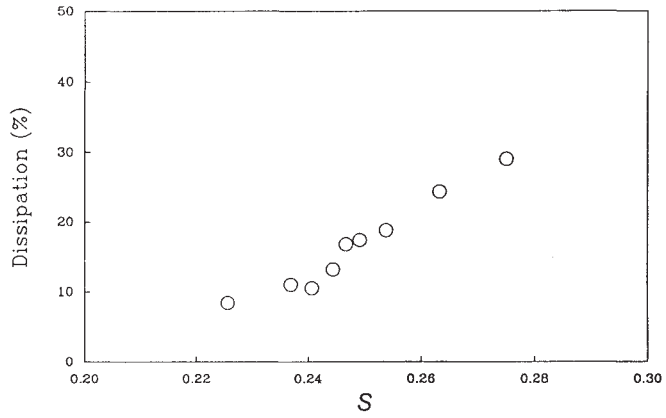

Fig. 1 Fractional dissipation of the energy in the wave packet as a function of the slope parameter S. The onset of breaking occurs at $S = 0.241$, and losses at lower values of S are due to other dissipation mechanisms in the channel (for example, viscous dissipation in the boundary layers). Note that to lowest order the fractional dissipation is equal to the fractional loss of excess momentum flux[1]. Each data point is the average of at least two repeats of the experiment.

Recently we have shown[1,2] that controlled experiments on breaking can be conducted in the laboratory and that the dissipation, turbulence and mixing resulting from breaking can be correlated with a few dimensionless variables that characterize the pre-breaking wave field. Of greatest importance is the fact that the dissipation, or momentum flux from waves to currents, depends most strongly on a dimensionless amplitude parameter, S, that describes the wave spectrum. Here $S = Na_ik_i$, where N is the number of spectral components, a_i is the amplitude of the component and $k_i = f_i^2/g$, with f_i the frequency of the component. In these experiments the slope a_ik_i of each component is held fixed, and we measure the radiated noise and microwave scattering from generated breaking waves.

Breaking waves were generated in a steel-framed glass channel 25 m long, 38 cm wide and 38 cm deep. A piston wave generator was programmed to focus a dispersive wave packet at a point 8 m down the channel. The wave packet was synthesized from 32 components of constant slope ak over a bandwidth of 0.64 Hz, spanning the range 0.56-1.2 Hz. The strength of breaking was controlled by varying the slope while keeping other parameters the same. The surface wave field was measured with an array of resistance wave gauges upstream and downstream of breaking, from which the dissipation resulting from breaking was determined as a function of the slope S (Fig. 1).

An X-band cw Doppler radar with a 15-cm aperture horn was mounted looking upstream (towards the oncoming waves). The wave channel was fitted with microwave-absorbing material to ensure that the only significant backscattering came from the surface waves. Preliminary experiments showed that at large angles of incidence multiple scattering was significant. To avoid this, we operated the radar at an incidence angle of 65°, with the aperture of the horn 71 cm above the quiescent water surface. The 3-db footprint of the radar extended 1 m along the water surface.

The sound generated by breaking was monitored with a B&K Model 8105 hydrophone mounted on an L-shaped support and pointing towards the breaking region. The hydrophone was kept

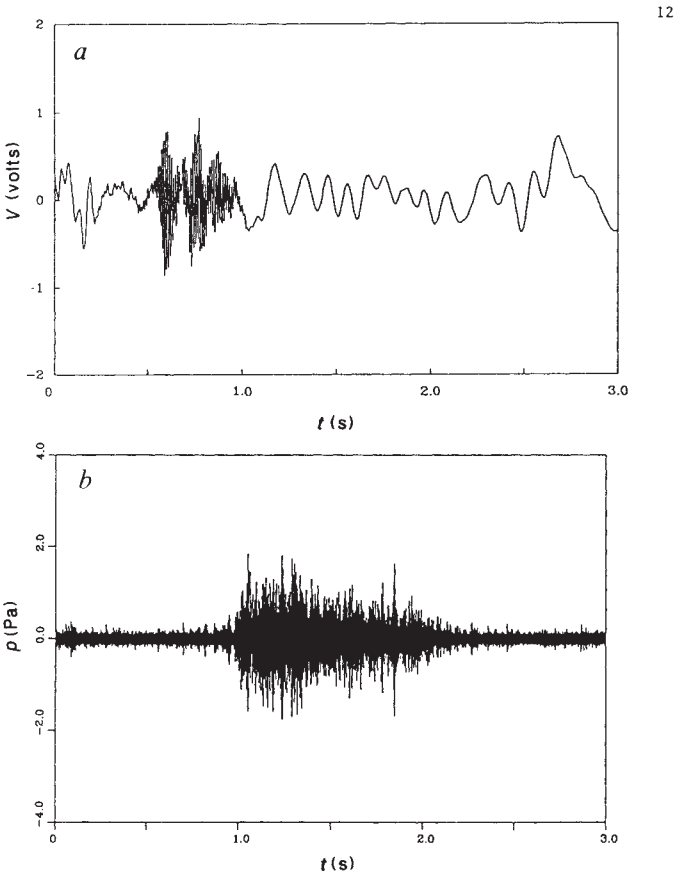

Fig. 2 Time series of the raw data measured for a typical breaker plunging at 7.5 m; $S = 0.254$. *a*, Radar backscatter measured at 8.5 m; *b*, Hydrophone signal measured at 15.5 m. Note the higher-frequency components which distinguish the breaking event in the radar signal. In subsequent figures the radar data has been band-passed in the range 50–250 Hz before additional processing.

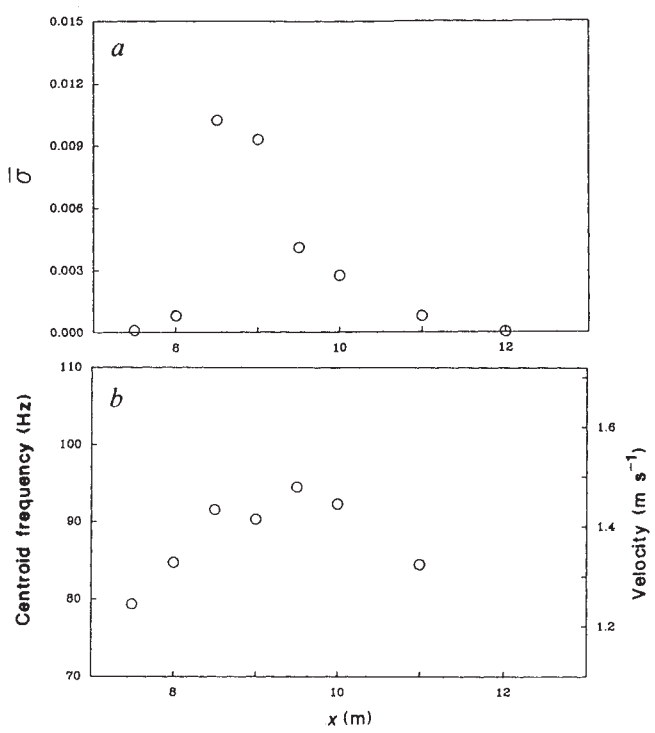

Fig. 3 *a*, Time-averaged radar backscattering cross-section, $\bar{\sigma}$ (in arbitrary units), for a plunging breaker ($S = 0.254$) measured at different locations along the tank. Each realization was averaged over 3 s. Three measurements were made at each position and ensemble averaged. *b*, Centroid frequency and corresponding horizontal velocity of the averaged Doppler spectrum for the measurements in *a*. Note that the determination of the centroid at $x = 12$ m was not meaningful as the band-passed signal was comprised almost entirely of 60-Hz noise and its harmonics.

at mid-depth to maximize the response to the lower acoustic modes. Measurements were made at a number of stations along the tank to account for attenuation along the channel. Surface gravity waves and acoustic waves were absorbed by a 'hog's hair' beach at the end of the channel. Tests showed that the reverberation time of the channel was ~100 ms, which is one order of magnitude less than the duration of the acoustic events that we measured. Preliminary measurements showed that the noise generated by breaking was divided between contributions at lower frequencies, up to 1,000 Hz, and those above the cutoff frequency at ~2,600 Hz. The lower-frequency components were contaminated by noise from the hydraulic wavemaker, so the measurements reported here were high-pass filtered at 500 Hz before digital sampling at 20 kHz. The wave-gauge signals were sampled at 100 Hz and the radar signal at 500 Hz.

For low values of S, breaking did not occur. On slowly increasing the slope a visual breaking threshold was obtained at $S = 0.241$. It was found that the visual and acoustic thresholds for breaking were coincident—that is, no acoustic event was observed below this visual threshold. But because capillary waves were generated on the forward face of steep (but unbroken) gravity waves, the radar scattering cross-section increased above the background noise level at values of S below the visual breaking threshold.

Figure 2 shows an example of the signals measured by the radar and the hydrophone for a single plunging event. The duration of each acoustic event was found to be within 15% of the duration of visible breaking at the surface. The duration of the breaking (high-frequency) event in the radar signal is shorter than that of the acoustic event but this is due in part to the fact that the footprint of the radar is shorter than the maximum length of the surface directly affected by breaking. The fact that the concave surface of the wave (immediately before breaking) is a good reflector may also contribute to the donation of the microwave event. To avoid difficulties associated with accounting for the antenna pattern of the radar and to arrive at a single measure of the backscatter from a breaking event, the radar measurements were taken at a number of positions along the channel. Spectral analysis of the radar data at values of S for which breaking occurred showed that the higher-frequency components associated with breaking could be isolated with a band-pass filter in the range 50–250 Hz. The 50-Hz lower limit offered a clear separation from the lower frequencies, which were associated with the orbital velocity components. Figure 3 shows an example of the measured radar cross-section as a function of position for a single breaking event, along with the centroid of the Doppler spectrum. The centroid is a measure of the mean velocity of the scatterers. In this case the centroid frequencies correspond to velocities in the range of the phase velocities of the components comprising the packet, 1.3–1.8 m s^{-1}. The cross-section is negligible outside the breaking region, so an unambiguous average backscattering cross-section may be measured.

To account for the attenuation of the acoustic modes along the channel, measurements were taken at a number of stations downstream of the breaking event. The mean-square pressure, p^2, decayed at an approximately constant rate along the channel, sensibly independent of S. For reasons of brevity we have chosen to display p^2 measured at 15.5 m, approximately four characteristic wavelengths downstream of the breakpoint. We have also integrated the time-averaged radar cross-section, $\bar{\sigma}$, along the channel to give a single space-time-averaged value, $\langle\bar{\sigma}\rangle$, for each event. Both p^2 and $\langle\bar{\sigma}\rangle$ are plotted as a function of S in Fig. 4*a*. These two variables are very strongly correlated and

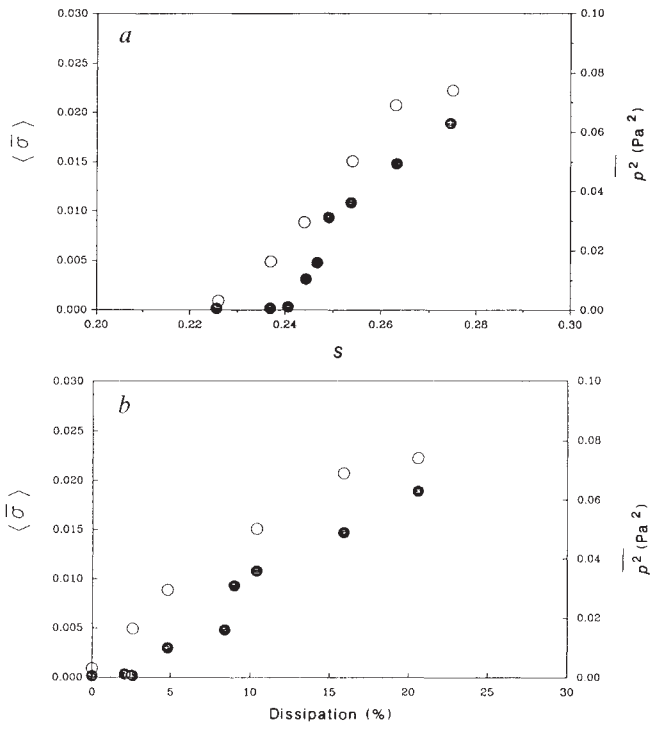

Fig. 4 *a*, The mean-square pressure, $\overline{p^2}$ (averaged over 4 s), (●) and the spatial average of the time-averaged radar cross-section, $\langle\bar{\sigma}\rangle$ (○), both plotted as a function of the slope parameter S. $\langle\bar{\sigma}\rangle = \int_{x_1}^{x_2} \bar{\sigma}\, dx$, where $\bar{\sigma}$ is given by results similar to Fig. 3*a*. *b*, p^2 and $\langle\bar{\sigma}\rangle$ (symbols as in *a*) re-plotted as functions of the fractional dissipation, using data from Figs 4*a* and 1.

both increase monotonically with S. The data from Figs 1 and 4*a* are combined in Fig. 4*b* to show the correlation of p^2 and $\langle\bar{\sigma}\rangle$ with the fractional dissipation (or loss of excess momentum flux through breaking)[1,2]. These data show that, within the scatter of the measurements, p^2 and $\langle\bar{\sigma}\rangle$ vary linearly with the dissipation that results from breaking.

These results show that both the noise generated by breaking and the radar cross-section of breaking waves can be correlated with important dynamical variables. In particular, if these results are shown to extend to the ocean, we anticipate that such measurements can be used to infer the dissipation and mixing from breaking at the ocean surface. For example, the data presented here would support the hypothesis that the radiated acoustic energy is proportional to the dissipated wave energy. Wilson[6] has proposed that the ambient noise in the ocean is proportional to the whitecap coverage, which is, in turn, approximately proportional to u_*^3, the cube of the friction velocity[7,8]. This would appear to be consistent with our measurements, which show that the acoustic energy radiated is approximately proportional to the gravity wave dissipation, which is also believed to scale with u_*^3. More precisely, we have found that the acoustic energy radiated is proportional to the duration and length of the breaking event which is the laboratory analogue of whitecap coverage.

We thank our colleagues in Electrical Engineering, MIT, MIT Lincoln Laboratory, and Bill Keller at NRL for advice and the loan of equipment. We thank Jack Croker for the design and construction of equipment, and Dr Tom Spence (formerly of ONR) for his support and encouragement during the initial stages of this research. This work was supported by an MIT/Sloan Grant, an ONR (Physical Oceanography) contract and an NSF grant to W.K.M. The participation of M.J.B. was supported by ONR (Arctic Programs).

Received 29 July; accepted 2 September 1988.

1. Melville, W. K. & Rapp, R. J. *Nature* **317**, 514–516 (1985).
2. Rapp, R. J. & Melville, W. K. *Phil. Trans. R. Soc. Lond.* (submitted).
3. Thorpe, S. A. *Phil. Trans. R. Soc. Lond.* **A304**, 155–210 (1982).
4. Farmer, D. M. & Vagle, S. *J. geophys. Res.* **93**, 3591–3600 (1988).
5. Phillips, O. M. *J. geophys. Res.* (in the press).
6. Wilson, J. H. *J. acoust. Soc. Am.* **63**, 952–956 (1980).
7. Monahan, E. C. & O'Muirheartaigh, I. G. *J. remote Sensing* **7**, 627–642 (1986).
8. Wu, J. *J. phys. Oceanogr.* **9**, 1064–1068 (1979).

Evidence from Fram Strait (78° N) for early deglaciation

Glenn A. Jones & Lloyd D. Keigwin

Woods Hole Oceanographic Institution, Woods Hole, Massachusetts 02543, USA

Recent syntheses of the history of the last Northern Hemisphere glaciation and deglaciation illustrate that understanding of the mechanisms and timing of deglaciation before approximately 12,000 years BP[1–5] is limited. After 12,000 yr BP, however, there is sufficient evidence from radiocarbon-dated moraines, raised beaches, varved lake sediments and pollen records to provide a reasonable temporal and geographic picture of the decay of the ice sheets. Here we report on the first oxygen isotope record from the Norwegian-Greenland Sea that is radiocarbon-dated directly by accelerator mass spectrometry. A significant light-oxygen-isotope event is recorded at approximately 15,000 years BP which suggests that the marine-based Barents Shelf ice sheet disintegrated rapidly at this time. Recent studies[6,7] have estimated that the decay of this ice sheet could have contributed as much as 15 metres to eustatic sea-level rise. The decay of the Barents Shelf ice sheet is the earliest major deglacial event yet dated, and may have triggered subsequent deglacial events through eustatic sea-level effects.

Boxcore PS21295-4, collected from the Fram Strait (Fig. 1) by the West German research vessel *Polarstern* in the summer of 1984, has a moderate sedimentation rate of 2.5 cm per 1,000 yr as defined by 22 accelerator mass spectrometry (AMS) ^{14}C analyses (Table 1 and Fig. 2). With the recent development of AMS it has become possible to date directly evidence of the last deglaciation in marine sediments[8–10]. Our core is a valuable northern endmember to those directly dated records published previously from 38° N off the coast of Portugal[9] and 55° N off Ireland[8]. The moderate sedimentation rate, the very young core-top age (<1,000 years) and the thin mixed layer (2–3 cm) indicate that resolution of palaeoceanographic events in our isotopic record is not likely to be degraded seriously by the effects of bioturbation.

It is generally believed that the glacial/interglacial ice-volume effect changed oceanic $\delta^{18}O$ by ~1.3‰ (refs 11, 12), but the glacial–interglacial amplitude of $\delta^{18}O$ recorded in planktonic foraminifera from most regions of the world's ocean averages ~1.6–1.7‰. In the North Atlantic, where isotopic records have been AMS-radiocarbon-dated previously, this amplitude approaches 2.5–3.0‰ (refs 8, 9). Enrichment of ^{18}O in excess of the 1.3‰ glacial–interglacial ice-volume signal is widely believed to be the result of the lower temperature of the sea water in which the foraminifera grew during glacial intervals. A 1 °C change in temperature results in a 0.23‰ change in the $\delta^{18}O$ recorded in calcite precipitated in the seawater[13], suggesting that some surface waters of the ocean were several degrees cooler during the last glaciation.

Fram Strait would be expected to preserve an isotope signal approximately equal in amplitude to the glacial–interglacial global-ice-volume signal with a minimal temperature overprint. Today this region is characterized by late-summer sea surface temperatures of ~2.0 °C (ref. 14). Taking into account the freezing point of sea water and the mechanisms of sea-ice formation, this region could have experienced no more than a 3.0 °C temperature depression between the last glacial maximum and today.